

# Metal-nonmetal transition and excitonic ground state in InAs/InSb quantum dots

Lixin He, Gabriel Bester, and Alex Zunger

National Renewable Energy Laboratory, Golden, Colorado 80401

(Dated: November 2, 2018)

Using atomistic pseudopotential and configuration-interaction many-body calculations, we predict a metal-nonmetal transition and an excitonic ground state in the InAs/InSb quantum dot (QD) system. For large dots, the conduction band minimum of the InAs dot lies below the valence band maximum of the InSb matrix. Due to quantum confinement, at a critical size calculated here for various shapes, the single-particle gap  $E_g$  becomes very small. Strong electron-hole correlation effects are induced by the spatial proximity of the electron and hole wavefunctions, and by the lack of strong (exciton unbinding) screening, afforded by the existence of fully discrete 0D confined energy levels. These correlation effects overcome  $E_g$ , leading to the formation of a bi-excitonic ground state (two electrons in InAs and two holes in InSb) being energetically more favorable (by  $\sim 15$  meV) than the state without excitons. We discuss the excitonic phase transition on QD arrays in the low dot density limit.

PACS numbers: 71.35.Lk, 73.21.La, 73.22.-f

The formation of excitons in semiconductors and insulators usually requires energy, e.g. photons, for one has to excite carriers across the single-particle band-gap  $E_g$ . There is a special interest, however, in the possibility of forming excitons exothermically, i.e. an “excitonic ground state” as envisioned by Mott [1] and Keldysh *et al.* [2]. Indeed, the electron-hole system exhibits a rich range of phases [3, 4] as a function of the carrier density and effective-mass ratio  $m_e/m_h$ , including various excitonic insulating states such as molecular solid, exciton liquid, Mott insulator, and also various metallic phases. The excitonic ground state is of fundamental interest in itself because excitons can be a better alternative to atoms for studying Bose-Einstein condensation[5, 6] on account of the lighter excitonic mass, thus higher condensation temperature. It is natural to search for excitonic ground states in systems where  $E_g$  is small, yet the screening is weak enough so as to prevent unbinding of the exciton. The search in *bulk solids* [7] has thus focused on *indirect* gap semiconductors and semimetals to reduce screening, but excitonic ground states have not been conclusively observed so far in such systems. Ground state excitons were also searched in *nanostructures*, specifically in spatially indirect quantum-wells [8, 9], where electrons and holes are confined in different spatial regions. In “type II” systems such as GaInAs/InP or CdTe/CdSe, electrons are localized in the well, whereas holes are localized on the barrier, so screening is weak, but  $E_g$  is finite. In contrast, in “type III” heterostructures such as [10] InAs/GaSb, the conduction band minimum (CBM) of the InAs well is lower than the valence band maximum (VBM) of the GaSb barrier, so at certain a well thickness one can have  $E_g \rightarrow 0$  [10], as well as separation of electrons from holes. Thus, at this thickness, one could expect an excitonic ground state if the electron-hole correlation energy will be large enough to stabilize the complex. Recent experiments [11] show evidence for existing excitonic ground state in type III InAs/Al<sub>x</sub>Ga<sub>1-x</sub>Sb quantum-well

superlattices; however, the binding energy was small (estimated at  $\sim 3$ -4 meV) and strong magnetic fields are needed to stabilize the system. This is because in a 2D periodic well or superlattice, extended states exist in the in-plane direction leading to rather weak excitonic binding.

The advantage of a type-III system can, however, be utilized without the disadvantage of 2D periodicity underlying a quantum-well, if one considers a type III *0D quantum-dot* (QD). The well-known InAs/Al<sub>x</sub>Ga<sub>1-x</sub>Sb epitaxial system [11] is inappropriate here, since it is lattice-matched, so dots will not form in a strain-induced Stranski-Krastanov (SK) growth [12]. We propose here a new dot matrix system, InAs/InSb, which has a type-III band alignment[13], and a lattice mismatch, and is hence amenable to epitaxial SK growth. Using an empirical pseudopotential approach [14], we find that as the dot size is reduced, electron levels localized on InAs move up in energy, whereas hole states, localized at the interface, initially above the electron levels, move down in energy. The system reaches a degeneracy  $E_g \sim 0$  of electron and hole single-particle levels at a critical size, predicted here for realistic dot shapes. As a result of the 0D confinement of both electrons and holes, there is but a small number of fully discrete bound states, so screening is limited. Using many-body configuration-interaction (CI), we find that consequently at the critical size, the exciton is bound by as much as  $\sim 15$  meV  $\gg E_g$ , thus forming an excitonic ground state. Our study characterizes theoretically the properties of the excitonic ground state in this system, offering experimentally testable predictions.

*Identifying the material system:* The customary way of selecting a *strained* dot/matrix system [12] is to require that the dot material has a smaller gap than the matrix material (e.g., InAs/GaAs or CdSe/ZnSe) so that all carriers can be confined inside the dot. In conventional semiconductors[15] the requirement  $E_g^{\text{dot}} < E_g^{\text{matrix}}$  im-

plies  $a^{\text{dot}} > a^{\text{matrix}}$ , where  $a$  is the bulk lattice constant, leading to compressive strain. Here, however, we seek  $E_g \rightarrow 0$  with spatially separated, yet confined carriers, so we might need a system where the CBM of the dot material is *below* the VBM of the matrix material. This could be met when the dot material has a *larger* band gap (thus, a smaller lattice constant) than the matrix material, leading to *tensile* strain. SK growth under tensile strain was demonstrated before for PbTe/PbSe[16]. The InAs/InSb system [10] has a lattice mismatch of  $\sim 7\%$ , and the CBM of InAs is below the VBM of InSb by 0.17 eV for the unstrained system. This guarantees that the electrons will be confined on InAs, and holes on InSb. We will see below that one can further chose a strained dot *shape* that will bring the holes to the interface, thus providing proximity, yet spatial separation of electrons and holes.

*Strain and confinement:* We have tested various dot shapes and sizes. Here we show three lens-shaped InAs dots of base/height = 104/26, 143/36 and 156/39 Å labeled as D1, D2 and D3, respectively, as well as spherical dots, all embedded in an InSb matrix. The supercell that includes the dot and the matrix contains up to about  $6 \times 10^5$  atoms. The strain is relaxed by minimizing the strain-energy with respect to the displacement of all atoms, representing the energy as a sum of bond-bending and bond-stretching force constants (the valence force field method (VFF) [17]). Denoting by  $\epsilon_{\alpha\beta}$ , the  $\alpha\beta$ -component of the strain tensor, Fig. 1(a) shows the strain profile along the (001) direction across the dot D2, demonstrating that the isotropic strain  $I = \epsilon_{xx} + \epsilon_{yy} + \epsilon_{zz}$  is positive (tensile), almost a constant inside the dots and decays to zero very rapidly in the barrier, whereas the biaxial component  $B = [(\epsilon_{xx} - \epsilon_{yy})^2 + (\epsilon_{yy} - \epsilon_{zz})^2 + (\epsilon_{zz} - \epsilon_{xx})^2]^{1/2}$  is nonzero and nonconstant inside the dot, but decays slowly to zero outside. To observe how this strain modifies the electronic properties, we show in Fig. 1(b) the strain-modified confining potentials obtained by inserting the strain of Fig. 1(a) into the Pikus-Bir equations[18]. The isotropic strain lowers both the CBM and the VBM of InAs, but the lowering of CBM is greater, leading to a large reduction of the gap from the unstrained bulk value of 0.42 eV to 0.01 eV. Very importantly, because of the curved shape of the strained dot leading to a large biaxial strain at the interface, the heavy-hole potential has a maximum at the InAs/InSb *interface*. We thus expect (and find below) that hole states will localize at the interface, rather than be extend throughout the barrier. This will enhance electron-hole binding.

*Method of calculation:* We relax the atomic position,  $\{\mathbf{R}_{n,\alpha}\}$  via the VFF method and construct the total pseudopotential of the system  $V(\mathbf{r})$  by superposing the local, screened atomic pseudopotential  $v_\alpha(\mathbf{r})$  of all (dot+matrix) atoms and the nonlocal spin-orbit poten-

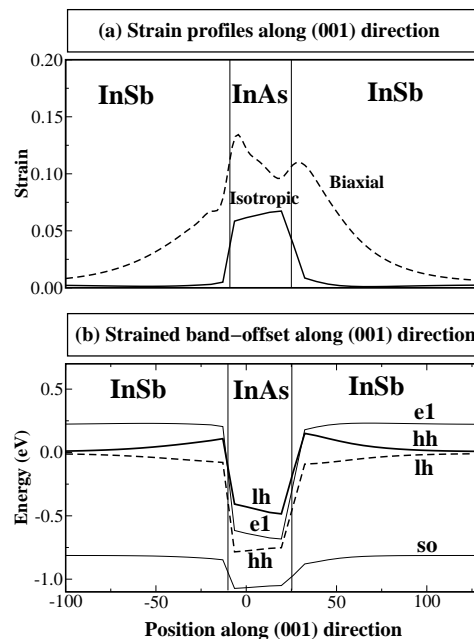


FIG. 1: (a) The isotropic and biaxial strain profiles along the (001) direction; (b) Strain-modified band-offset along (001) direction calculated from Pikus-Bir model. **e1**, **hh**, **lh** and **so** denote the band characters of the confining potential.

tials  $V_{\text{SO}}$ :  $V(\mathbf{r}) = V_{\text{SO}} + \sum_{n,\alpha} v_\alpha(\mathbf{r} - \mathbf{R}_{n,\alpha})$ . We use the Linear Combination of Bulk Bands (LCBB) method [19], where the Hamiltonian  $-1/2\nabla^2 + V(\mathbf{r})$  is diagonalized in a basis  $\{\phi_{m,\epsilon,\lambda}(\mathbf{k})\}$  of Bloch orbitals of band index  $m$  and wave vector  $\mathbf{k}$  of material  $\lambda$  ( $=$  InAs, InSb, GaAs), strained uniformly to strain  $\epsilon$ . This LCBB approach [19] produces accurate results for many nanostructures [20], and greatly surpasses in accuracy the  $\mathbf{k} \cdot \mathbf{p}$  method which limits the basis to  $m = \text{VBM} + \text{CBM}$  at  $\mathbf{k} = 0$  only. The pseudopotentials of Ref. 13 are used for InAs/InSb with minor modifications [21]. Many-body effects are included via the configuration interaction (CI) method[22] by expanding the total wavefunction in Slater determinants for single and bi-excitons formed from all of the confined single-particle electron and hole states. The Coulomb and exchange integrals are computed numerically from the pseudopotential single-particle states, using the microscopic position-dependent dielectric constant [22]. Our CI approach is very similar to the Bethe-Salpeter equations[23], except that in the latter case all the exchange integrals are unscreened, whereas since the exchange potential has a long-range component [22], we do allow its screening.

*Single-particle states:* Diagonalization of the atomistic single-particle pseudopotential Hamiltonian gives the confined single-particle electron and hole energy levels shown in Fig. 2. The corresponding wavefunctions for D2 are shown in Fig. 3. We see that the four InAs-confined electron states e1, e2, e3, e4 move *down* in en-

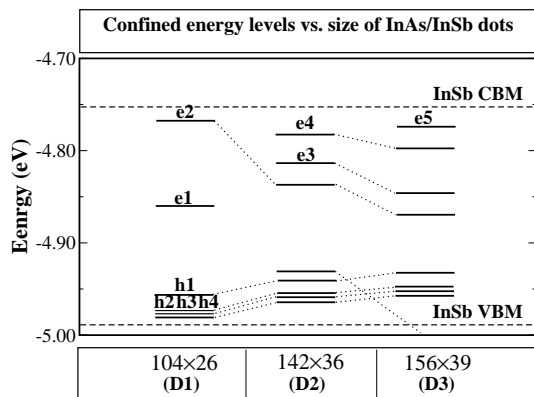


FIG. 2: Single-particle spectrum of D1 ( $104 \text{ \AA} \times 26 \text{ \AA}$ ), D2 ( $142 \text{ \AA} \times 36 \text{ \AA}$ ), D3 ( $156 \text{ \AA} \times 39 \text{ \AA}$ ). e1, e2, e3, e4 are the InAs-confined electron states, while h1, h2, h3, h4 are localized hole states.

ergy as the dot size increases; whereas the interfacially confined (see. Fig. 3) hole states h1 and h2 move *up* in energy as the size increases. For the smallest dot D1, there is a finite, single-particle gap of 96 meV between the first confined electron and hole states. For dot D2, the gap reduces to  $\sim 6$  meV. For the large dot D3, the lowest InAs-confined electron level lies *below* the VBM of the InSb barrier and hybridizes with it. The single-particle gap is thus negative, signaling a charge transfer from InSb to InAs.

*Many-body states:* The energies were carefully converged by increasing the basis in the many-body expansion. For an uncorrelated electron-hole pair, the energy is  $E_g$ , whereas correlation could reduce the energy of the monoexciton  $E_X$  by  $\Delta_X \equiv E_g - E_X$ . Bi-excitons  $E_{XX}$  could be bound with respect to two excitons by  $\Delta_{XX} \equiv 2E_X - E_{XX}$ . The CI energies are shown in Fig. 4. The results show that for dot D1,  $E_X=79$  meV and  $E_{XX}=161$  meV both positive i.e, correlation energies do not overcome the single-particle gap. However, for dot D2 we find that correlation reduces the energy of the single electron-hole pair from 6 meV to  $E_X = -9$  meV, whereas for two electron-hole pairs, the reduction is from 12 meV to  $E_{XX} = -15$  meV. Thus, both mono- and bi-excitons are now stable, the bi-exciton being the ground state, lower in energy than the “no exciton” case of a fully occupied valence bands and fully empty conduction bands state. To see whether the shape of the dot affects these conclusions, we performed similar calculations for spherical InAs/InSb QDs. The critical diameter for the metal-nonmetal transition is now around  $2R=64 \text{ \AA}$ . The calculated exciton and bi-exciton energies are shown in Fig. 4(b) for two diameters ( $52 \text{ \AA}$  and  $64 \text{ \AA}$ ). For the  $2R=64 \text{ \AA}$  dot, we find an exciton energy of  $E_X = -22$  meV, and a bi-exciton energy of  $E_{XX} = -39$  meV. Again the bi-exciton is the ground state.

*Properties of excitonic ground state:* For lens-shaped

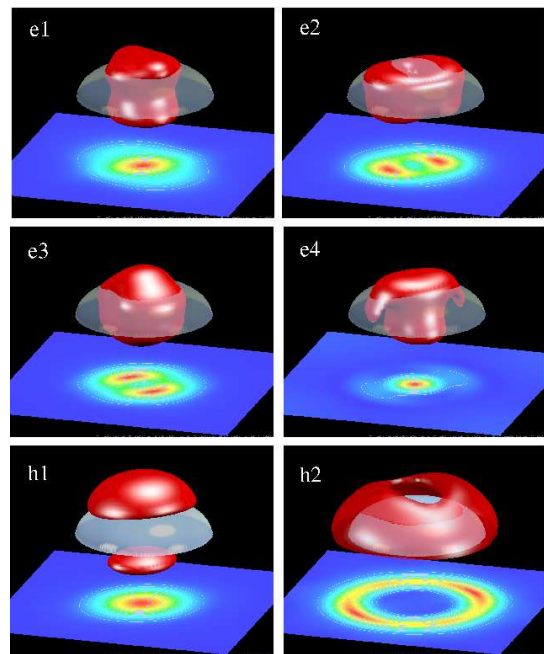


FIG. 3: COLOR: Wavefunction of the InAs-confined electron states (e1-e4) and the first two hole states (h1-h2). The transparent lenses indicate the positions of InAs dots. The isosurface enclose 50 % of the state density except for e4 which is only weakly confined. For e4, the isosurface enclose only about 10 % of the state density. The contour plot are slices of the density taken from chosen planes.

dots, the monoexciton binding energy  $\Delta_X$  are 17 and 15 meV for dot D1 and D2 respectively, whereas the negative bi-exciton binding energy of  $\Delta_{XX} = -3$  meV for both D1 and D2, indicating an unbound bi-exciton. For the spherical dot with  $2R=64 \text{ \AA}$ ,  $\Delta_X = 19$  meV and  $\Delta_{XX} = -5$  meV. The bi-exciton is also unbound. The bi-excitonic ground state is similar to a helium atom in the sense that there are two positive and two negative Coulomb bound charges. These states can be identified as “excitonic molecule” states [4]. The calculated permanent electric dipole moment  $\mathbf{p} = \int \mathbf{x}\rho(\mathbf{x})d^3x$  for the exciton and bi-exciton of the lens-shaped dot D2 are aligned along (001) direction (growth direction), and amount to  $p_z=3.58 \text{ e\AA}$  for the exciton and  $p_z=7.16 \text{ e\AA}$  for the bi-exciton. These dipoles could be measured experimentally and since the exciton binding energy is so high ( $\sim 15$  meV), it can be studied at rather high temperatures.

Given these excitonic dipoles, it is interesting to study the collective behavior of excitons in the QD arrays due to dipolar interactions. Recent developments in epitaxial growth made it now possible to grow arrays of QDs [24]. At a *low dot density*, where the QDs are far apart, the excitons behave like in the single dot while couple only weakly via dipole-dipole interactions. For simplicity, we ignore the fine structure [20] of the excitons and assume there can be only one exciton per dot at most (the results

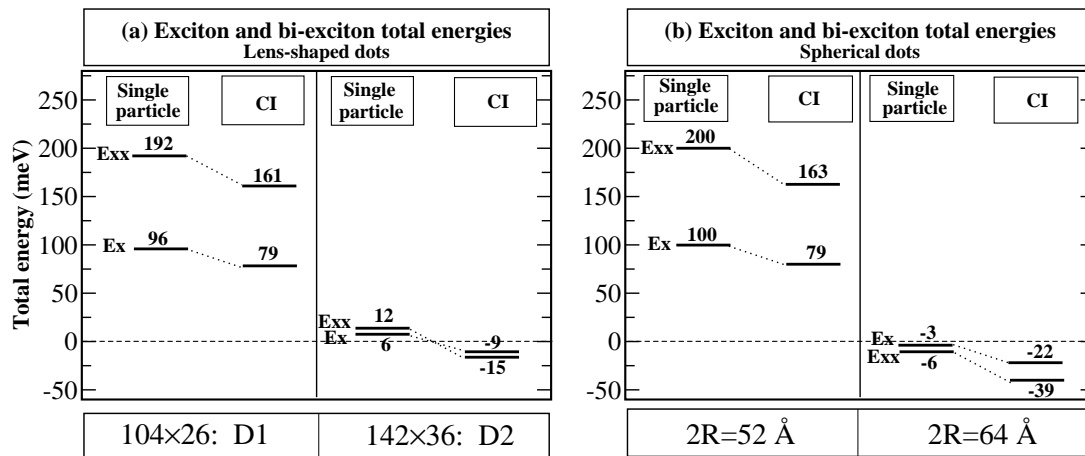


FIG. 4: Exciton and Bi-exciton energies of (a) lens-shaped, and (b) spherical, InAs dots embedded in InSb matrix.

can be easily generalized to the case allowing two excitons per dot). The excitonic phase transition can be described using an Ising-like Hamiltonian,

$$H = E_X(\eta) \sum_i n_i + \frac{1}{2} \sum_{i,j} J_{ij}(\eta) n_i n_j,$$

where,  $n_i$  is the number of excitons on dot  $i$ , and its value can be either 0 or 1.  $E_X(\eta)$  is the formation energy of an exciton on a single dot, which is a function of  $\eta$  being dot size, density etc. The dipole-dipole interaction  $J_{ij}$  between the exciton on site  $i$  and site  $j$  is a function of both dot density and array structures. We consider here the case where the average interaction  $\langle J \rangle = 1/2N \sum_{i,j} J_{ij}(\eta) < 0$  (ferromagnetic-like), where  $N$  is the total number of QDs in the array. At  $T=0$  K, when  $E(\eta) + \langle J \rangle < 0$ , all QDs are occupied by excitons, thus the ground state is an *excitonic state*, accompanied by a macroscopic dipole moment. When  $E(\eta) + \langle J \rangle > 0$ , no exciton will form in the QDs lattice, resulting in the *normal* insulating state. Particular interesting is the quantum critical point, where  $E(\eta) + \langle J \rangle = 0$ . Here the fully occupied excitonic state and the fully empty state have the same energy, and the state could be either excitonic or normal, which can be switched by applying an electric field. However, at a critical temperature  $T_c$ , there are large fluctuations between these two states leading to large fluctuations of dipole moment. Furthermore, the size distribution and disorder of the QDs lattice may lead to more complicated “Bose glass” phase [25, 26].

At *medium and high* densities, where the QDs have stronger coupling, there could be numerous phases as a function of carrier density and mass ratios, as proposed in Ref. 4. In these regions, the picture of (bi-)exciton on a single QD is not valid anymore. However, the electron-hole density and mass ratio can be tuned via the parameters of dots arrays, such as the size and confining potential of a single dot, the density of dots, and even

the structure of the dots arrays, thus make them very promising for studying the electron-hole phase diagram.

To conclude, our pseudopotential many-body calculations predict a valence-to-conduction single-particle energy level cross-over and a spontaneous formation of bi-excitonic ground state at the critical size of lens-shaped and spherical InAs/InSb dot system. There are two reasons that make this type-III QD system a very promising candidate for studying excitonic ground state. First, the electron-hole energy gap is tunable by the QDs size alone, and second, the excitons have much larger binding energies than in the bulk, or QW due to the 0D confinement for both electrons and holes. Experimental studies on such a proposed excitonic ground-state are called for.

We thank R. Magri for providing us with the InAs and InSb pseudopotentials. This work was supported by US DOE-SC-BES-DMS, grant no. DEAC36-98-GO10337.

- 
- [1] N. F. Mott, Phil. Mag. **6**, 287 (1961).
  - [2] L. V. Keldysh and Y. V. Kopayev, Fiz. Tverd. Tela **6**, 2791 (1964) [ Sov. Solid State **6**, 2219 (1965)]; L. V. Keldysh and A. N. Kozlov, Zh. Eksp. Teor. Fiz, **54**, 978 (1968) [ Sov. Phys. JETP **27**, 521 (1968)].
  - [3] B. I. Halperin and T. M. Rice, Rev. Mod. Phys. **40**, 755 (1968).
  - [4] P. B. Littlewood, G. J. Brown, P. R. Eastham, and M. H. Szymanska, Phys. Stat. Sol. (b) **234**, 36 (2002).
  - [5] A. Griffin, D. W. Snoke, and S. Stringari, eds., *Bose-Einstein Condensation* (Cambridge university press, 1995).
  - [6] L. V. Butov, C. W. Lai, A. L. Lvanov, A. C. Gossard, and Chemla, Nature **417**, 47 (2002).
  - [7] B. Bucher, P. Steiner, and P. Wachter, Phys. Rev. Lett. **67**, 2717 (1991).
  - [8] S. Datta, M. R. Melloch, and R. L. Gunshor, Phys. Rev. B **32**, 2607 (1985).
  - [9] X. Zhu, P. B. Littlewood, M. S. Hybertsen, and T. M.

- Rice, Phys. Rev. Lett. **74**, 1633 (1995).
- [10] R. Magri, L. W. Wang, A. Zunger, I. Vurgaftman, and J. R. Meyer, Phys. Rev. B **61**, 10235 (2000).
- [11] J. P. Cheng, J. Kono, B. D. McCombe, I. Lo, W. C. Mitchel, and C. E. Stutz, Phys. Rev. Lett. **74**, 450 (1995).
- [12] D. Bimberg, M. Grundmann, and N. N. Ledentsov, *Quantum Dot Heterostructures* (John Wiley & Sons, 1999).
- [13] R. Magri and A. Zunger, Phys. Rev. B **65**, 165302 (2002).
- [14] A. Zunger, phys stat. sol (b) **224**, 727 (2001).
- [15] O. Madelung, ed., *Landolt-Börnstein*, vol. 22a (Springer-Verlag Berlin Heidelberg, 1987).
- [16] M. Pinczolits, G. Springholz, and G. Bauer, Appl. Phys. Lett. **73**, 250 (1998).
- [17] P. N. Keating, Phys. Rev. **145**, 637 (1966).
- [18] G. E. Pikus and G. L. Bir, Phys. Rev. Lett. **6**, 103 (1961).
- [19] L.-W. Wang and A. Zunger, Phys. Rev. B **59**, 15806 (1999).
- [20] G. Bester, S. V. Nair, and A. Zunger, Phys. Rev. B **67**, 161306 (2003).
- [21] The InSb pseudopotentials are revised to reproduce correct band-offset of InSb VBM relative to GaSb, changing it from 40 meV below the GaSb VBM to 34 meV above one.
- [22] A. Franceschetti, H. Fu, L.-W. Wang, and A. Zunger, Phys. Rev. B **60**, 1819 (1999).
- [23] G. Onida, L. Reining, and A. Rubio, Rev. Mod. Phys. **74**, 601 (2002).
- [24] Q. Xie, A. Madhukar, P. Chen, and N. Kobayashi, Phys. Rev. Lett. **75**, 2542 (1995).
- [25] J. A. Hertz, L. Fleishman, and P. W. Anderson, Phys. Rev. Lett. **43**, 942 (1979).
- [26] M. P. Fisher, P. B. Weichman, G. Grinstein, and D. S. Fisher, Phys. Rev. B **40**, 546 (1989).